Chinese Journal of Cardiology
Volume 54 Issue 3, Year of Publication 2026, Page 182-196 | DoI-10.545120/0253-3758.2026.044

ISSN : 0253-3758
DOI: ***10.545120/0253-3758***

Available online at
https://cjcardiology.com

Chinese Journal of Cardiology
cjcardiology.com

Development and Characterization of Pitavastatin–Ion Exchange Resin Complex for Effective Taste Masking

Shivam D. Parekh [1], Suraj R. Chauhan[2], Jitendra O. Bhangale[3]
[1]Student, Smt. N. M. Padalia Pharmacy College, Ahmedabad, Gujarat, 382210, India;
[2]Associate Professor, Smt. N. M. Padalia Pharmacy College, Ahmedabad, Gujarat, 382210, India;
[3]Professor and Principal, Smt. N. M. Padalia Pharmacy College, Ahmedabad, Gujarat, 382210, India.
*Corresponding Author E-mail: **jitu2586@gmail.com**

Article Information
Received: 22-12-2025
Revised: 19-01-2026
Accepted: 17-02-2026
Published: 26-03-2026

KEYWORD:
Pitavastatin, Ion-exchange resin, Taste masking, Fast disintegrating tablets.

ABSTRACT:
The present study aimed at the development and characterization of a Pitavastatin–ion exchange resin complex to achieve effective taste masking and improved drug release for hyperlipidaemia management. Pitavastatin, a BCS Class II drug with poor aqueous solubility and bitter taste, was complexed with ion-exchange resins using optimized formulation conditions. Preformulation studies confirmed drug identity and purity with melting point 189–193 °C and λ_{max} at 249 nm. The calibration curve (2-10 ppm) demonstrated excellent linearity (R^2 = 0.9992), validating the analytical method. Drug–resin complexes were prepared using Indion 204 and Indion 234 resins and optimized for drug loading. Maximum drug loading 80.57% was achieved at a drug–resin ratio of 1:3 with Indion 204, indicating superior ion-exchange efficiency. The optimized complex was further formulated into fast disintegrating tablets and evaluated for physicochemical parameters and *In-Vitro* drug release. Among all batches, formulation PSF7 exhibited nearly complete drug release (99.58%) within 12 mins. along with desirable disintegration characteristics. Thus, the developed formulation successfully achieved taste masking, controlled drug release, and improved patient compliance, demonstrating its potential as an effective oral delivery system.

INTRODUCTION:

Cardiovascular diseases remain a major global health concern, with high cholesterol especially LDL cholesterol being a key risk factor. Although several lipid-lowering drugs are available, maintaining long-term control is still difficult due to issues like poor patient compliance, inconsistent drug absorption, and side effects. From a formulation standpoint, there is a clear need to develop drug delivery systems that improve bioavailability, ensure controlled release, and enhance patient adherence.[1-2]

Pitavastatin, a third-generation statin, was chosen for this study because of its strong cholesterol-lowering effect and lower risk of drug interactions. However, its clinical use is limited by poor water solubility, variable bioavailability, first-pass metabolism, and a bitter taste, all of which can reduce patient acceptance especially in patient-friendly dosage forms.[3]

To overcome these challenges, complexation with an ion-exchange resin was explored as an effective strategy for taste masking and controlled drug release. In this approach, the drug remains bound in the mouth, preventing bitterness, and is gradually released in the gastrointestinal tract, improving drug availability and reducing fluctuations in plasma levels. Incorporating this complex into fast disintegrating tablets further enhances convenience, particularly for geriatric and dysphagic patients, by allowing rapid disintegration without water. Overall, this formulation approach offers a promising way to improve both therapeutic performance and patient

compliance. [4-5]

MATERIALS AND METHOD:

Materials: Excipients like Indion 204, Indion 234, Crospovidone, MCC, PVP K30, Talc, Magnesium Stearate were obtained from Chemdyes Corporation, Rajkot, Gujarat, India.

Formulation Method of Drug Ion Exchange Resin Complex (DRC)

A. Selection of resin: The selection of resins was guided by the properties of the drug and specific formulation requirements. Generally, the choice between cation and anion exchange resins is determined by whether the drug exhibits acidic or basic characteristics. For Pitavastatin, which is a weakly acidic drug contributing to its bitterness, weak cation exchange resins were chosen. Indion 204 and Indion 234 are pharmaceutical-grade ion-exchange resins containing carboxylic functional groups, which exhibit weak acid cation-exchange characteristics. These resins are widely used in oral formulations for taste masking and drug–resin complexation. Although Pitavastatin is a weakly acidic drug, effective complexation can occur under optimized pH conditions through ionic and secondary interactions within the resin matrix. The porous structure and good exchange capacity of Indion 204 and Indion 234 facilitate efficient drug loading and stable complex formation. Their established pharmaceutical use and experimental drug-loading performance justify their selection for developing Pitavastatin ion-exchange resin complexes.[6-7]

B. Preparation of drug resin complex (DRC): For the preliminary study, a drug-to-resin ratio of 1:1 was used. An accurately measured quantity of resin was placed in a beaker with 25 ml of deionized water and allowed to swell for 30 minutes. The appropriate amount of drug, based on the 1:1 ratio, was then added, and the solution's pH recorded. The mixture was stirred on a magnetic stirrer at 30°C for 30 minutes. After stirring, the solution was filtered with Whatman filter paper, and the filtrate was analyzed - following appropriate dilution - to measure unbound drug content using a UV spectrophotometer. The residue on the filter was dried in a hot air oven at 40 °C. The percentage of drug bound to the resin was calculated based on the amount of unbound drug. This process was repeated for each resin type individually. Later the DRCs were optimized for drug loading capacity. [8-9]

3^2 Factorial Design for optimization: A 3^2 full factorial design was employed to optimize the formulation of fast disintegrating tablets containing the Pitavastatin–ion exchange resin complex, with Crospovidone concentration (X_1) and PVP K30 concentration (X_2) selected as independent variables, each studied at three levels (−1, 0, +1). These variables were chosen based on their known influence on tablet disintegration and drug release behavior. The design generated nine experimental formulations, and their impact was assessed on critical response variables including *In-Vitro* disintegration time, wetting time, and cumulative percentage drug release at 2 and 12 minutes. The experimental data were subjected to ANOVA using Design Expert software, and a quadratic polynomial model incorporating main effects, interaction terms, and quadratic components was developed to establish a meaningful relationship between the formulation variables and the measured responses. This statistically driven approach not only minimized the number of experiments required but also provided a reliable framework for predicting and fine-tuning formulation performance, ultimately guiding the development of an optimized tablet formulation with rapid disintegration and efficient drug release characteristics.[10-11]

Direct Compression Method for Preparation of Fast Disintegrating Tablets: Fast disintegrating tablets of Pitavastatin were prepared using the direct compression method due to its simplicity, cost-effectiveness, and suitability for moisture- and heat-sensitive formulations.

Initially, the accurately weighed quantity of Pitavastatin–ion exchange resin complex was taken and passed through a suitable sieve (e.g., #60) to ensure uniform particle size. All excipients were also sieved separately to remove lumps and ensure uniformity. The sieved ingredients were then mixed thoroughly using geometric dilution to achieve a homogeneous blend. After uniform mixing, lubricants such as talc and magnesium stearate were added to the blend and mixed gently for a short duration to avoid over-lubrication, which could affect tablet hardness and disintegration. The final powder blend was evaluated for pre-compression parameters. Subsequently, the blend was directly compressed into tablets using Cronimach lab scale rotary tablet compression machine with 8 mm punch to obtain tablets of uniform weight. This method ensured minimal processing steps, uniform drug distribution, rapid

disintegration, effective taste masking, and overall improved patient compliance. [12-13]

Table 1: Formulation of Fast Disintegrating tablet using 3^2 Factorial design

Ingredients (mg)	PSF1	PSF2	PSF3	PSF4	PSF5	PSF6	PSF7	PSF8	PSF9
Pitavastatin IER	14.84	14.84	14.84	14.84	14.84	14.84	14.84	14.84	14.84
Avicel pH 102	30	30	30	30	30	30	30	30	30
Crospovidone	2.4	2.4	2.4	4.2	4.2	4.2	6	6	6
PVP K 30	1.2	2.4	3.6	1.2	2.4	3.6	1.2	2.4	3.6
D-mannitol	64.4	63.2	62.0	62.6	61.4	60.2	60.8	59.6	58.4
Aspartame	2.4	2.4	2.4	2.4	2.4	2.4	2.4	2.4	2.4
SLS	1.2	1.2	1.2	1.2	1.2	1.2	1.2	1.2	1.2
Talc	2.4	2.4	2.4	2.4	2.4	2.4	2.4	2.4	2.4
Magnesium stearate	1.2	1.2	1.2	1.2	1.2	1.2	1.2	1.2	1.2
Total weight	**120**	**120**	**120**	**120**	**120**	**120**	**120**	**120**	**120**

PREFORMULATION STUDIES

Determination of Melting point of Pitavastatin: The melting point of Pitavastatin was determined using a melting point apparatus (Popular, India). A small amount of the drug was placed in a thin-walled capillary tube sealed at one end. The capillary tube was then placed in a melting point apparatus with a thermometer, and the temperature range over which Pitavastatin melted was recorded. The measurements were taken in triplicate.[14]

Estimation of Pitavastatin by UV-Visible Spectrophotometry: The estimation of Pitavastatin was carried out using UV–Visible spectrophotometry (Shimadzu 1900) in a simple and systematic manner. A standard stock solution (100 µg/ml) was first prepared by dissolving 10 mg of the drug in 100 ml of phosphate buffer pH 6.8. The maximum absorption wavelength (λ_{max}) was then determined by scanning the solution between 200–400 nm, where Pitavastatin showed maximum absorbance at 249 nm. Working solutions (2-10 ppm) were prepared by appropriate dilution of the stock solution. The absorbance of each solution was measured three times at 249 nm using phosphate buffer pH 6.8 as the blank to ensure accuracy and reproducibility. Overall, this method provides a simple, reliable, and precise approach for the quantitative estimation of Pitavastatin.[15-16]

FTIR: FTIR was performed for determination of Pitavastatin and was estimated for standard FTIR peaks.[17] FTIR spectroscopy of pure drug and physical mixture of drug and excipients was carried out to check the compatibility of drug and excipients.[18]

Optimization of various conditions for maximum drug loading capacity: To ensure that Pitavastatin was loaded onto the resin as efficiently as possible, a series of formulation conditions were carefully studied and optimized one by one. To begin with, the effect of resin activation was examined by treating the resin separately with 1N HCl and 1N NaOH, washing it thoroughly with deionized water until a neutral pH was achieved, and then comparing the drug loading efficiency obtained with acid-activated and alkali-activated resin. Following this, the drug-to-resin ratio was explored by combining 500 mg of Pitavastatin with different amounts of resin ranging from 0.5 to 2 gm in 100 ml of deionized water, stirring the mixture for 4 hours, and then filtering and assessing the drug content. The role of pH in influencing drug loading was then investigated by preparing drug-resin complexes at several pH levels between 1.2 and 7, which were adjusted using standard solutions of HCl and NaOH. The impact of temperature was studied by carrying out the drug loading process at five different temperatures, from 20°C to 60°C, with the help of a temperature-controlled magnetic stirrer. To find the ideal swelling time for the resin, it was allowed to hydrate in deionized water for different time intervals of 30, 60, 90, and 120 minutes before proceeding with drug loading. Lastly, the stirring time was optimized by preparing the drug-resin complex under continuous stirring for durations ranging from 30 to 300 minutes. At each of these conditions, the % drug loading efficiency was calculated to pinpoint the most favorable parameters for preparing a well-optimized drug-resin complex.[19-20]

Drug Content: A complex equivalent to 4 mg was accurately weighed and 10 ml of phosphate buffer pH 6.8 was added to break the drug:resin complex, under continuous stirring for 2 mins. Solution was filtered and absorbance was measured at 249 nm using UV-spectrophotometer the readings were taken in triplicate.[19-20]

Chinese Journal of Cardiology
Volume 54 Issue 3, Year of Publication 2026, Page 182-196 | DoI-10.545120/0253-3758.2026.044

EVALUATION PARAMETERS FAST DISINTEGRATING TABLET

Precompression Parameters

Bulk density: Carefully weigh the powder mixture and transfer it to a measuring cylinder. Measure the volume of the powder without applying pressure. The volume is expressed as grams per milliliter (gm/ml).[21-22]

$$\text{Bulk Density} = \frac{\text{Mass of powder (gm)}}{\text{Bulk Volume of powder (ml)}}$$

Tapped density: The tapped density was determined by placing a graduated cylinder containing the formulation blend on a mechanical tapping apparatus. The volume was tapped until a constant tapped volume was achieved. Tapped density is expressed as grams per milliliter (gm/ml).[21-22]

$$\text{Tapped Density} = \frac{\text{Mass of powder (gm)}}{\text{Tapped Volume of powder (ml)}}$$

Hausner's ratio: Hausner's ratio, determined by dividing the tapped density by the bulk density of a powder, serves as an indicator of powder flow. A ratio at or below 1.25 signifies favorable flow properties, while a ratio surpassing 1.25 indicates inadequate flow. [21-22]

$$\text{Hausner's ratio} = \frac{\text{Tapped density}}{\text{Bulk density}}$$

Compressibility index: The compressibility index is a percentage value obtained by calculating the difference between the tapped density and bulk density of a material, then dividing this difference by the tapped density. It serves as a measure of the compressibility or ability of a powder to decrease in volume under pressure. [21-22]

$$\text{Compressibility Index} = \frac{\text{Tapped density} - \text{Bulk density}}{\text{Tapped density}} \times 100$$

Angle of repose: Angle of repose was determined by funnel method. Powder blend was poured from funnel that can be raised vertically until it reaches maximum cone height (h) was obtained. Radius (r) of the pile was measured. Angle of repose was measured by following formula. [21-22]

$$\text{Tan}\,\theta = \frac{h}{r} \qquad \theta = \tan^{-1}\frac{h}{r}$$

Where, θ = Angle of repose, h = Height of pile, r = Radius of pile

Post Compression Parameters

Thickness: Thickness of the tablets were gauged using Digimatic Vernier Calipers. Five tablets were selected at random, and their thickness and diameter were measured by positioning them between the two arms of the Vernier calipers.[23]

Hardness: Tablet hardness is characterized as the force needed to fracture a tablet in a diametric compression examination. The crushing strength of tablets was assessed using a Monsanto-type hardness tester. [23]

Weight variation: Twenty tablets were randomly picked from each batch and weighed one by one using a calibrated analytical balance, following the guidelines set by the Indian Pharmacopoeia. The average weight was then calculated, and how much each tablet deviated from this average was worked out in percentage terms. Since the prepared tablets had a total weight of 120 mg, the IP-specified acceptable deviation limit of ± 7.5% was considered for evaluation, and all results were expressed as mean ± standard deviation.[23]

Friability test: The friability of tablets was assessed using a Roche-type friabilator. Initially, twenty tablets were weighed, and subsequently, they were placed in the friabilator, operated at 25 rpm for 4 minutes. Afterward, the tablets were removed and weighed again. The loss in weight should not exceed 1%. The percentage of friability was determined using the following equation.[24]

$$\%\ \text{Friability} = \frac{\text{Initial weight} - \text{Final weight}}{\text{Initial weight}} \times 100$$

Drug content: 10 tablets were weighed, and their average weight was computed, crushed in a mortar and powder, equivalent to 4 mg of Pitavastatin, was dissolved in a small quantity of Phosphate buffer pH 6.8. The drug solution was filtered through Whatman filter paper and examined for drug content using UV Spectrophotometry at 249 nm after appropriate dilutions. [25]

Wetting time: Six circular tissue papers, each with a diameter of 10 cm, were placed in a petri dish. A solution consisting of 10 ml of phosphate buffer with a pH of 6.8, containing amaranth dye, was added to the petri dish. Following this, a tablet was delicately positioned on the surface of the tissue paper. The time it took for the liquid to reach the upper surface of the tablet was noted as the wetting time. [25]

***In-Vitro* Disintegration test:** The test involved using a digital tablet disintegration test apparatus (Bhawna India) to assess 3 tablets. Phosphate buffer with a pH of 6.8, maintained at a temperature of 37 ± 0.5 °C, served as the disintegration media. The time taken, measured in seconds, was recorded for the tablets to completely disintegrate, leaving no residue in the apparatus. [25]

***In-Vitro* Drug release study:** The % of drug release from Pitavastatin Fast Disintegrating tablet was assessed using the USP type II dissolution apparatus (DKB Instruments), operating at 50 rpm and maintained at 37° ± 0.5°C with 900 ml of phosphate buffer (pH 6.8). Samples were withdrawn at regular intervals, replaced with fresh dissolution media, and filtered through a 0.45µm membrane filter. The absorbance of these samples was analyzed using a UV at a wavelength of 249 nm. [25]

Stability study of optimized batch: In this study, the stability of the optimized batch was assessed under accelerated conditions of 40°C ± 2°C and 75% ± 5% relative humidity (RH) for a duration of one month. The formulation was wrapped in aluminum foil to shield it from light exposure as per ICH guidelines. After the 30-day period, tablets were analyzed for hardness, drug content, and *In-vitro* drug release.[26]

RESULTS AND DISCUSSION:

Preformulation Study:

Determination of Melting point of Pitavastatin: Melting point determination, a commonly employed technique for drug identification, was conducted using a melting point apparatus, revealing a range of 189 - 193 °C for Pitavastatin. This falls within the reported melting point range of 190 - 192 °C for Pitavastatin. Consequently, it was inferred that the provided substance is indeed Pitavastatin.

Estimation of drug by UV overlay spectra

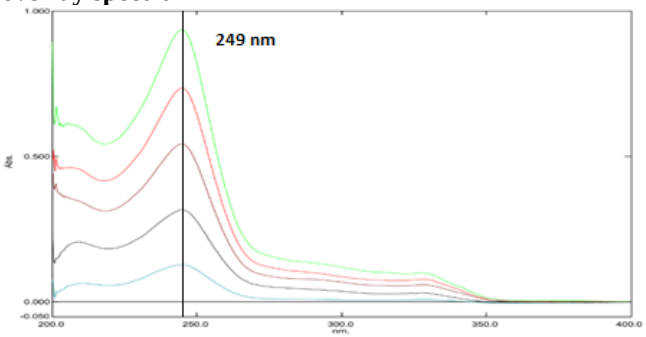

Figure 1: Overlay Spectra of Pitavastatin

The superimposed spectra of the drug were generated by scanning various solution concentrations, including 2, 4, 6, 8, and 10 ppm, revealing peak absorption at 249 nm. Since the reported λ_{max} for Pitavastatin is 249-250 nm, it can be deduced that the provided substance is indeed Pitavastatin.

Analytical Method for Pitavastatin:

The absorbance of Pitavastatin in a phosphate buffer at pH 6.8 was assessed using a UV-Visible spectrophotometer

across a wavelength range of 200−400 nm, with a notable maximum absorption (λ_{max}) observed at 249 nm. For the construction of a calibration curve, working solutions spanning concentrations from 2 to 10 ppm were prepared from the Pitavastatin stock solution in the phosphate buffer at pH 6.8. The prepared Pitavastatin solutions were analyzed for absorbance at λ_{max} (249 nm) against a blank of phosphate buffer at pH 6.8 using a UV−Visible Spectrophotometer. A calibration curve was then constructed by plotting the concentration against absorbance (Figure 2).

Table 2: Absorbance of different concentration of Pitavastatin in pH 6.8 phosphate buffer

Sr. No.	Concentration (ppm)	Absorbance			Mean Absorbance ± S.D.
		I	II	III	
1	2	0.125	0.131	0.128	0.128 ± 0.0030
2	4	0.309	0.316	0.328	0.318 ± 0.0096
3	6	0.535	0.542	0.551	0.543 ± 0.0080
4	8	0.729	0.735	0.743	0.736 ± 0.0070
5	10	0.942	0.949	0.931	0.961 ± 0.0091

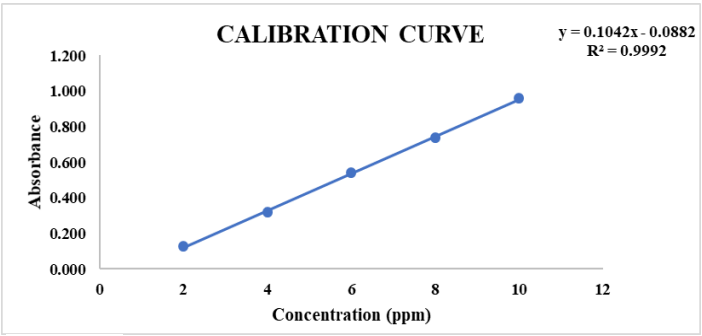

Figure 2: Calibration curve of Pitavastatin in phosphate buffer at pH 6.8

FTIR Study of Pitavastatin & Drug-Excipients Compatibility study

FTIR spectroscopy was carried out to confirm the identity of Pitavastatin, and the resulting spectrum displayed all the key absorption bands typical of its functional groups, which matched well with the reference standard. This gave a clear confirmation that the drug was genuine and correctly identified. To check whether any of the excipients could potentially interact with the drug, physical mixtures of Pitavastatin with excipients was analyzed by FTIR. On comparing these spectra with that of the pure drug, it was reassuring to find that all the major peaks remained intact at their original positions, with no meaningful changes in their shape, intensity, or location. No new peaks appeared in the mixture spectra, which is a strong indication that none of the excipients triggered any unwanted chemical reaction with Pitavastatin. Overall, these results build confidence that Pitavastatin is well compatible with the chosen excipients in the development of stable and effective tablet formulations.

EVALUATION OF DRUG ION RESIN COMPLEX

Optimization of various conditions for maximum drug loading: Drug loading process was optimized for maximum drug loading considering conditions like effect of activation, drug: resin ratio, pH, temperature, resin swelling time and stirring time.

Optimization of Drug-Resin Ratio: The effect of drug-to-resin ratio on percentage drug loading was studied for both Indion 204 and Indion 234 resins, some clear and interesting trends came to light as shown in table 3. At lower resin concentrations, drug loading was noticeably poor, which was not surprising given that fewer ion-exchange sites were available to accommodate the drug molecules. As the resin proportion was gradually increased, drug loading picked up steadily, pointing towards better and more productive interaction between the drug and the resin. The sweet spot was found at a 1:3 drug-to-resin ratio, where Indion 204 delivered a loading efficiency of 80.57% and Indion 234 followed with 72.33%. Pushing the resin content beyond this point did not bring any further benefit and instead caused a drop in drug loading, most likely because the excess resin was not being utilized effectively. Given that Indion 204 consistently outperformed Indion 234 across the studied ratios, it was the natural choice to carry forward for further optimization studies.

Table 3: Effect of Drug-Resin ratio on Drug loading

Drug-Resin ratio	% Drug Loading	
	Indion 204	**Indion 234**
1:1.0	46.64	43.69
1:1.5	49.67	46.49
1:2.0	59.29	56.22
1:2.5	61.53	60.41
1:3.0	**80.57**	72.33
1:3.5	73.09	69.91
1:4.0	58.23	52.52

Optimization of Resin Activation: The effect of resin activation method on drug loading efficiency was studied at a fixed drug-to-resin ratio of 1:3, and the results turned out to be quite telling as shown in table 4. Acid-activated resin came out on top with the highest drug loading of 81.09%, which can be attributed to the effective protonation of functional groups that made more ion-exchange sites readily available for drug interaction. Alkali-activated resin, on the other hand, performed noticeably lower at 70.20%, likely because the alkaline environment reduced the affinity between the drug and the resin. The resin that underwent combined acid-alkali activation fell somewhere in between, achieving a drug loading of 77.39%, suggesting only a partial recovery of ion-exchange capacity. All things considered, acid activation clearly proved to be the most effective approach for maximizing drug loading, and was therefore carried forward as the preferred activation method for subsequent formulation studies.

Table 4: Effect of Resin activation on Drug loading

Resin Activation	Drug Resin Ratio	% Drug Loading
1:3	**ACID**	**81.09**
1:3	**ALKALI**	70.20
1:3	**ACID-ALKALI**	77.39

Optimization of pH: The influence of pH on drug loading efficiency was evaluated across a range of pH values, and the results clearly pointed towards a pH-dependent behavior. At strongly acidic conditions (pH 1.2–2), drug loading was relatively low, likely because excess hydrogen ions competed with drug molecules for the available resin binding sites. As pH was gradually raised from 3 to 5, drug loading improved steadily, reflecting better ionization of the drug and stronger interaction with the resin. The highest drug loading of 84.03% was recorded at pH 5.5, indicating that this condition offered the most favorable ion-exchange environment. A marginal drop in drug loading was observed at pH 6, possibly due to a reduction in binding affinity at higher pH levels. Based on these findings, pH 5.5 was identified as the optimum pH for achieving maximum drug loading and was adopted for further studies.

Table 5: Effect of pH on Drug loading

pH	% Drug Loading
1.2	41.01
2	44.04
3	56.80
4	67.64
5	74.94
5.5	**84.03**
6	80.60

Optimization of Temperature: The effect of temperature on drug loading on resin was shown in table 6. The effect of temperature on percentage drug loading was evaluated to identify the optimum conditions for drug–resin complexation. At 20 °C, moderate drug loading (69.7%) was observed, indicating limited molecular mobility. Increasing the temperature to 30 °C resulted in a marked increase in drug loading (89%), suggesting enhanced diffusion of drug molecules and improved interaction with the resin. However, further elevation of temperature led to a gradual decline in drug loading. At 40 °C, drug loading decreased slightly to 84.4%, while a significant reduction was observed at 50 °C (68.4%) and 60 °C (59.6%). This reduction at higher temperatures may be attributed to weakening of electrostatic interactions or partial desorption of the drug from the resin. Therefore, 30 °C was identified as the optimum temperature for achieving maximum drug loading.

Table 6: Effect of temperature on Drug loading

Temperature (ºC)	% Drug Loading
20	69.73
30	**88.95**
40	84.36
50	68.44
60	59.58

Optimization of resin swelling time: The influence of swelling time on percentage drug loading was evaluated to determine the optimal hydration period for effective drug–resin complexation as shown in table 7. At a swelling time of 30 min, moderate drug loading (71.23%) was observed, indicating incomplete resin hydration. Increasing the swelling time to 60 min resulted in improved drug loading (74.67%), suggesting enhanced availability of ion-exchange sites. Maximum drug loading (83.14%) was achieved at 90 min, indicating optimal swelling and effective drug diffusion into the resin matrix. Further increase in swelling time led to a decline in drug loading, with values of 76.32% at 120 min and 68.29% at 150 min. The reduction at prolonged swelling times may be attributed to overhydration, leading to dilution of binding sites or partial drug desorption. Therefore, a swelling time of 90 min was identified as optimal for maximum drug loading.

Table 7: Effect of swelling time on Drug loading

Drug-Resin ratio	Swelling Time (min)	% Drug Loading
1:3	**30**	71.23
1:3	**60**	74.67
1:3	**90**	**83.14**
1:3	**120**	76.32
1:3	**150**	68.29

Optimization of resin stirring time: The effect of stirring time on percentage drug loading was investigated to optimize the drug–resin complexation process as shown in table 8. At a stirring time of 30 min, relatively low drug loading (69.5%) was observed, which may be attributed to insufficient contact between the drug and resin. Increasing the stirring time to 60 min resulted in a slight improvement in drug loading (71.14%), indicating enhanced interaction. Maximum drug loading (88.1%) was achieved at a stirring time of 120 min, suggesting optimal exposure of ion-exchange sites and effective diffusion of drug molecules into the resin matrix. However, further increase in stirring time led to a decline in drug loading, with values of 74.39% at 150 min and 70.47% at 180 min. This decrease may be due to saturation of binding sites or partial desorption of the drug. Thus, a stirring time of 120 min was considered optimal.

Table 8: Effect of Stirring time on Drug loading

Drug-Resin ratio	Stirring time (min)	% Drug Loading
1:3	**30**	69.5
1:3	**60**	71.14
1:3	**90**	80.63
1:3	**120**	**88.1**
1:3	**150**	74.39
1:3	**180**	70.47

A systematic optimization of the drug–resin complex was carried out using Indion 204 and Indion 234 by studying the effects of drug–resin ratio, resin activation method, pH, temperature, swelling time, and stirring time on percentage drug loading. Among the two resins evaluated, Indion 204 consistently exhibited higher drug loading than Indion 234, indicating superior ion-exchange capacity. Maximum drug loading was obtained at a drug–resin ratio of 1:3, while acid activation of the resin produced significantly higher loading compared to alkali and acid–alkali activation. Drug loading increased with pH and reached an optimum at pH 5.5, after which a slight decline was observed. Temperature optimization revealed 30 °C as the most favorable condition for effective drug–resin interaction. Additionally, a swelling time of 90 min and a stirring time of 120 min were found to be optimal for maximizing drug loading. Based on the overall evaluation, the acid-activated Indion 204 resin at a 1:3 drug–resin ratio, prepared at pH 5.5 and 30 °C with 90 min swelling and 120 min stirring, was selected as the optimized drug–resin complex for further formulation development.

RESULTS OF FAST DISINTEGRATING TABLETS PREPARED BY USING DRC OF PITAVASTATIN

PRECOMPRESSION PARAMETERS

Table 9: Bulk density, Tapped density, Carr's index, Hausner's ratio and Angle of Repose data

Batch	Bulk density (gm/ml)	Tapped density (gm/ml)	Carr's index (%)	Hausner's Ratio	Angle of repose (°θ)
PSF1	1.72 ± 0.021	1.92 ± 0.169	9.68 ± 7.945	1.11 ± 0.094	26.69 ± 0.620
PSF2	1.74 ± 0.021	1.92 ± 0.163	9.21 ± 8.730	1.11 ± 0.102	26.74 ± 0.153
PSF3	1.75 ± 0.037	1.95 ± 0.181	10.11 ± 6.977	1.12 ± 0.083	26.89 ± 0.867
PSF4	1.80 ± 0.030	2.00 ± 0.175	9.40 ± 7.775	1.11 ± 0.092	26.53 ± 0.294
PSF5	1.82 ± 0.030	2.01 ± 0.160	8.91 ± 8.587	1.10 ± 0.100	25.90 ± 0.328
PSF6	1.83 ± 0.047	2.04 ± 0.180	9.88 ± 6.080	1.11 ± 0.072	26.86 ± 0.516
PSF7	1.89 ± 0.025	2.09 ± 0.174	9.11 ± 7.446	1.11 ± 0.088	26.08 ± 0.388
PSF8	1.91 ± 0.025	2.10 ± 0.166	8.60 ± 8.302	1.10 ± 0.096	27.78 ± 0.352
PSF9	1.92 ± 0.037	2.13 ± 0.180	9.54 ± 6.307	1.11 ± 0.074	27.12 ± 0.625

The pre-compression evaluation of powder blends (PSF1–PSF9) indicated good overall flow and compressibility characteristics suitable for tablet formulation. The bulk density values (1.72–1.92 g/mL) suggested efficient initial packing of the powders, while the higher tapped density values (1.92–2.13 g/mL) reflected proper particle rearrangement upon tapping. The Carr's compressibility index (8.60–10.11%) and Hausner's ratio (1.10–1.12) further confirmed that most formulations possessed excellent to good flow properties with minimal cohesiveness. In addition, the angle of repose values (25.90°–27.78°), being well below 30°, clearly indicated excellent flow behavior. Overall, these results demonstrate that all powder blends were uniform, free-flowing, and well-suited for direct compression into tablets.

POST COMPRESSION PARAMETERS

Table 10: Weight variation, Thickness, Hardness and Friability data

Batch	Weight variation (mg)	Thickness (mm)	Hardness (kg/cm^2)	Friability
PSF1	120.75 ± 1.410	3.27 ± 0.058	3.57 ± 0.029	0.62 ± 0.27
PSF2	121.20 ± 1.105	3.17 ± 0.058	3.72 ± 0.134	0.65 ± 0.19
PSF3	120.60 ± 1.231	3.30 ± 0.000	3.85 ± 0.131	0.66 ± 0.22
PSF4	120.90 ± 1.334	3.27 ± 0.058	3.31 ± 0.127	0.68 ± 0.10
PSF5	121.20 ± 1.361	3.27 ± 0.058	3.40 ± 0.006	0.73 ± 0.19
PSF6	120.45 ± 1.504	3.33 ± 0.058	3.47 ± 0.115	0.77 ± 0.17
PSF7	120.80 ± 1.436	3.33 ± 0.058	2.93 ± 0.112	0.80 ± 0.18
PSF8	121.35 ± 1.268	3.30 ± 0.000	3.12 ± 0.103	0.81 ± 0.40
PSF9	120.75 ± 1.552	3.27 ± 0.058	3.20 ± 0.200	0.84 ± 0.31

Table 11: Drug content, Wetting time and invitro disintegration time data

Batch	% Drug content	Wetting time (sec.)	In vitro Disintegration time (sec.)
PSF1	99.12 ± 0.699	30.39 ± 0.60	33.26 ± 0.74
PSF2	96.35 ± 0.925	34.05 ± 0.60	36.81 ± 1.09
PSF3	99.43 ± 0.200	36.34 ± 0.46	39.49 ± 0.62
PSF4	99.18 ± 0.604	23.03 ± 0.49	25.88 ± 0.83
PSF5	96.72 ± 0.560	25.78 ± 0.49	29.00 ± 0.41
PSF6	97.44 ± 0.545	28.36 ± 0.36	30.94 ± 0.65
PSF7	99.16 ± 0.634	13.54 ± 0.67	16.71 ± 0.64
PSF8	98.26 ± 0.260	18.66 ± 0.81	21.74 ± 0.82
PSF9	99.70 ± 0.290	20.48 ± 0.49	23.41 ± 0.58

The evaluation results of the fast disintegrating tablets of pitavastatin prepared using an ion exchange resin complex indicate that all formulations (PSF1–PSF9) exhibited satisfactory and uniform quality characteristics.

The **Weight Variation** of all batches remained within a narrow range (120.45–121.35 mg), confirming good flow properties of the powder blend and uniform die filling during compression. The thickness (3.17–3.33 mm) was consistent across batches, reflecting uniform tablet dimensions.

The **Hardness** values (2.93–3.85 kg/cm²) indicate that the tablets possessed adequate mechanical strength while still being suitable for fast disintegration. All formulations showed friability below 1% (0.62–0.84%), demonstrating sufficient resistance to mechanical stress and good handling properties.

The **Drug Content** ranged from 96.35% to 99.70%, confirming uniform drug distribution throughout the formulations and compliance with acceptable limits.

A significant variation was observed in **Wetting Time** (13.54–36.34 seconds) and ***In-Vitro* Disintegration Time** (16.71–39.49 seconds), which are critical parameters for fast disintegrating tablets. Among all batches, PSF7 showed the best performance, with the lowest wetting time (13.54 sec) and disintegration time (16.71 sec), indicating rapid tablet hydration and breakdown.

Overall, all formulations met the required evaluation criteria; however, PSF7 was identified as the optimized formulation, offering the most desirable balance between tablet strength and rapid disintegration, making it highly suitable for fast disintegrating tablet development.

Table 12: Percentage drug release of batches PSF 1 to PSF 9

Time (min.)	PSF1	PSF2	PSF3	PSF4	PSF5	PSF6	PSF7	PSF8	PSF9
0	0	0	0	0	0	0	0	0	0
2	30.92	26.82	23.88	36.18	33.12	29.58	47.58	44.09	40.31
4	50.18	44.92	40.76	57.82	54.08	48.69	73.09	68.41	64.04
6	66.02	60.74	56.38	74.92	70.58	64.83	90.08	86.03	81.62
8	80.62	75.79	70.88	88.87	85.18	79.71	98.21	96.37	93.58
10	88.12	84.19	79.63	94.28	91.81	88.57	99.31	98.57	97.08
12	92.37	89.58	85.42	96.61	94.96	93.18	99.58	99.12	98.27

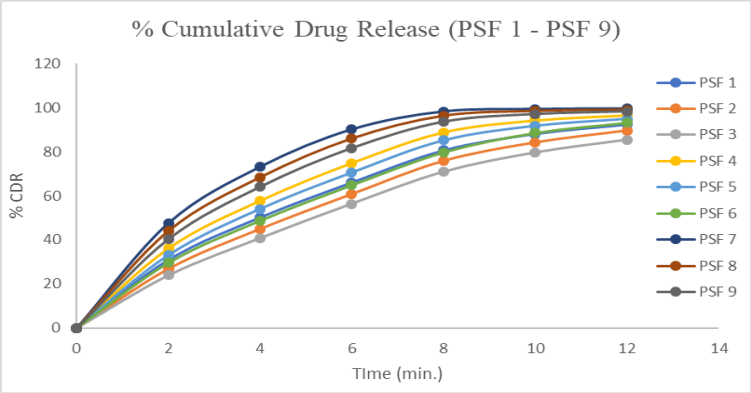

Figure 3: % *In-vitro* Cumulative drug release of Batches PSF 1 to PSF 9

% *In-Vitro* Cumulative Drug release: The *In-Vitro* dissolution profiles of formulations PSF1 to PSF9 were evaluated over a 12-minute study period. At the initial time point, drug release varied across batches, with PSF7 showing the fastest onset of release. As the study progressed, all formulations demonstrated a steady rise in cumulative drug release, though notable differences in release rates were observed among the batches. PSF7 consistently outperformed the other formulations, achieving 90.08% release at 6 minutes and reaching as high as 99.58% by the end of 12 minutes. Formulations PSF8 and PSF9 also showed comparatively faster release, while PSF2 and PSF3 exhibited a relatively slower dissolution pattern throughout the study. By the 12-minute mark, all formulations had achieved considerable drug release, ranging from 85% to 99.58%. These findings clearly suggest that the formulation composition played a significant role in governing the dissolution behavior, and PSF7 was identified as the optimized batch owing to its rapid and most efficient drug release profile.

Chinese Journal of Cardiology
Volume 54 Issue 3, Year of Publication 2026, Page 182-196 | DoI-10.545120/0253-3758.2026.044

STATISTICAL ANALYSIS OF VARIOUS DEPENDENT VARIABLES

Statistical Analysis for Y_1 (Wetting Time): The polynomial equation obtained for wetting time ($Y_1 = 26.26 + 3.04B_1 - 8.02B_2 + 0.2475B_{12} - 0.8067B_1^2 - 0.1467B_2^2$) revealed that Crospovidone concentration (X_1) had a positive influence, while PVP K30 concentration (X_2) showed a negative effect on wetting time. The contour plot (Figure 4a) and 3D response surface plot (Figure 4b) collectively demonstrated that lower concentrations of Crospovidone combined with higher levels of PVP K30 resulted in reduced wetting time, indicating faster wetting of the tablets. Conversely, higher Crospovidone concentrations with lower PVP K30 levels led to prolonged wetting time. The predicted versus actual plot (Figure 4c) showed that the data points were closely scattered along the diagonal line, confirming a strong agreement between the predicted and experimentally observed values, and validating the reliability and good predictive ability of the developed model.

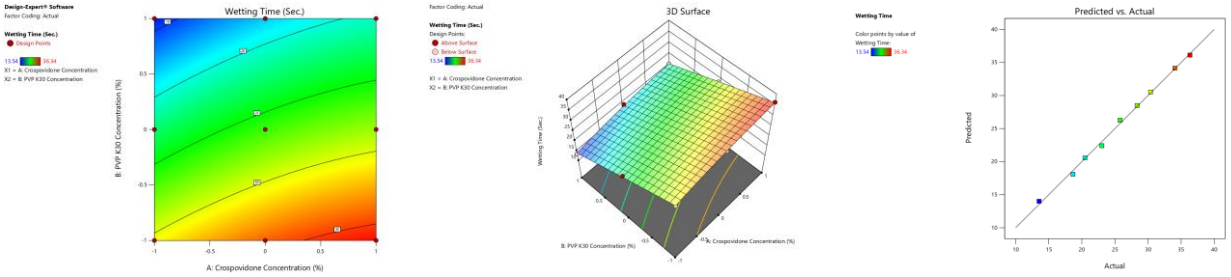

a **b** **c**

Figure 4: (a) Contour plot showing the effect of Crospovidone (%) (X_1) and PVP K30 (%) (X_2) on wetting time (sec.) (b) 3D surface plot showing the effect of Crospovidone (%) (X_1) and PVP K30 (%) (X_2) on Wetting time (sec.) (c) Graph of Actual value vs Predicted value for Wetting time (sec.)

Statistical Analysis for *In-vitro* Disintegration time (sec.): The polynomial equation for *In-Vitro* disintegration time ($Y_2 = 26.26 - 3.04B_1 - 8.02B_2 + 0.2475B_{12} - 0.8067B_1^2 - 0.1467B_2^2$) indicated that both Crospovidone concentration (X_1) and PVP K30 concentration (X_2) carried negative coefficients, meaning that raising the levels of either excipient contributed to a reduction in disintegration time. Among the two, PVP K30 appeared to exert a more pronounced effect owing to its larger coefficient value. The contour plot (Figure 5a) illustrated that the shortest disintegration times were achieved in regions where both Crospovidone and PVP K30 concentrations were at their higher levels, as represented by the cooler blue zones in the plot. The 3D response surface (Figure 5b) further reinforced this trend, displaying a gradual decline in disintegration time as the concentrations of both variables were increased, forming a smooth and well-defined surface. The predicted versus actual plot (Figure 5c) presented a neat alignment of data points along the reference diagonal, reflecting excellent agreement between the model predictions and the experimental observations. This close correspondence between predicted and actual values demonstrates that the model is well-fitted and capable of reliably predicting *In-Vitro* disintegration time within the studied design space.

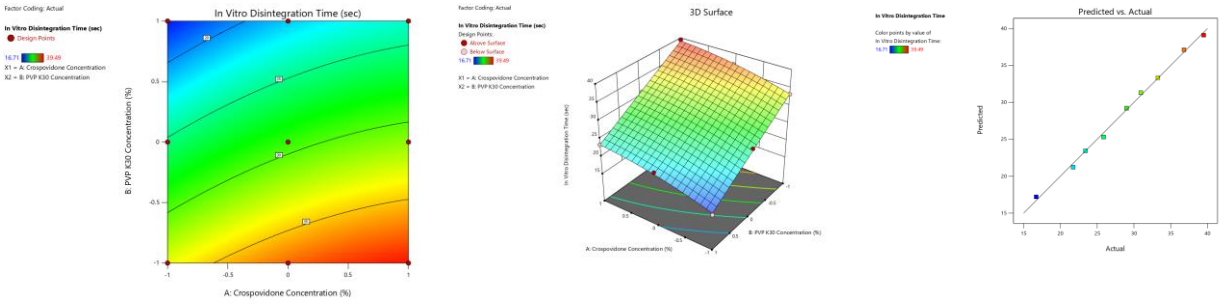

a **b** **c**

Figure 5: (a) Contour plot showing the effect of Crospovidone (%) (X_1) and PVP K30 (%) (X_2) on *In-vitro* Disintegration time (sec.) (b) 3D surface plot showing the effect of Crospovidone (%) (X_1) and PVP K30 (%) (X_2) on *In-vitro* Disintegration time (sec.) (c) Graph of Actual value vs Predicted value for *In-vitro* Disintegration time (sec.)

Statistical Analysis for Y_3 (% CDR at 2 mins.): The polynomial equation for % CDR at 2 minutes ($Y_3 = 32.92 -$

$3.49B_1 + 8.39B_2 - 0.0575B_{12} + 0.0650B_1^2 + 2.64B_2^2$) made it quite clear that the two formulation variables influenced drug release in opposite ways. While Crospovidone concentration (X_1) tended to pull drug release down with its negative coefficient, PVP K30 concentration (X_2) worked in the other direction, actively boosting early drug release and doing so more strongly, as its positive coefficient was noticeably larger. Looking at the contour plot (Figure 6a), it was easy to see that the highest % CDR values were found in areas where PVP K30 concentration was high and Crospovidone was relatively low, with the color gradient transitioning from cooler to warmer shades as drug release improved. The 3D response surface plot (Figure 6b) brought this relationship to life even more vividly, showing a clear upward rise in % CDR as PVP K30 levels increased, making the individual and combined effects of both variables straightforward to understand visually. To top it all off, the predicted versus actual plot (Figure 6c) showed that the model performed very well, with the data points sitting neatly along the diagonal reference line throughout the entire value range, which is a strong sign that the model is reliable and capable of accurately predicting % CDR at 2 minutes across the experimental design space.

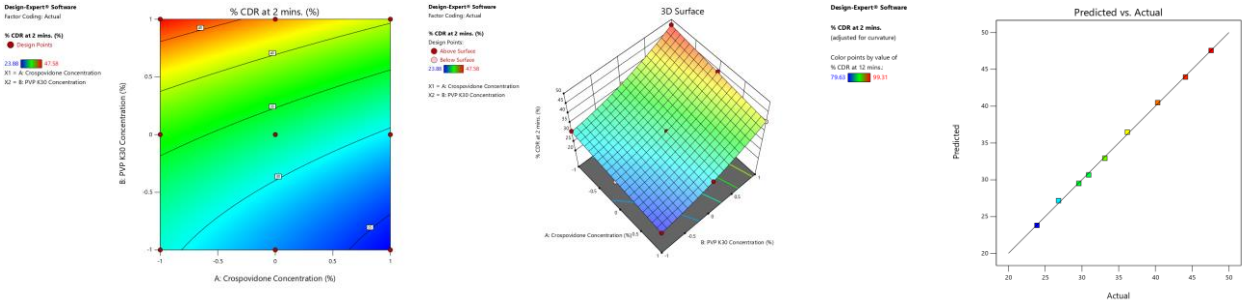

a **b** **c**

Figure 6: (a) Contour plot showing the effect of Crospovidone (%) (X_1) and PVP K30 (%) (X_2) on % CDR at 2 mins. (b) 3D surface plot showing the effect of Crospovidone (%) (X_1) and PVP K30 (%) (X_2) on % CDR at 2 mins. (c) Graph of Actual value vs Predicted value for % CDR at 2 mins.

Statistical Analysis for Y_4 (% CDR at 12 mins.): The polynomial equation for % CDR at 12 minutes ($Y_4 = 91.79 - 2.74B_1 + 7.17B_2 + 1.56B_{12} - 0.3583B_1^2 - 0.4033B_2^2$) painted an interesting picture of how the two formulation variables shaped drug release by the end of the dissolution study. Crospovidone concentration (X_1) appeared to work against complete drug release with its negative coefficient, while PVP K30 concentration (X_2) took the lead in pushing drug release higher, and its noticeably larger positive coefficient made it clear that it was the more influential of the two variables. Glancing at the contour plot (Figure 7a), the pattern was fairly straightforward to read the warmer red and orange shades indicating higher % CDR were concentrated in areas where PVP K30 levels were high and Crospovidone concentrations were on the lower side, while the cooler blue tones at the opposite corner of the plot pointed to reduced drug release. The 3D response surface plot (Figure 7b) added another layer of clarity to this story, showing a smooth and steady upward trend in % CDR as PVP K30 concentration climbed, making it visually intuitive to grasp how the two variables worked together to determine the final dissolution outcome. Perhaps most importantly, the predicted versus actual plot (Figure 7c) gave good reason to trust the model, as the experimental data points tracked the diagonal reference line very faithfully throughout the entire range, leaving little gap between what the model predicted and what was actually observed.

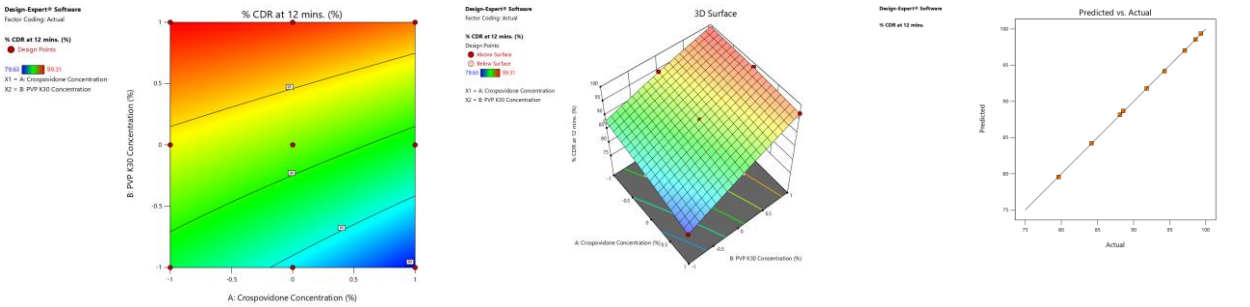

a **b** **c**

Figure 7: (a) Contour plot showing the effect of Crospovidone (%) (X_1) and PVP K30 (%) (X_2) on % CDR at 12 mins. (b) 3D surface plot showing the effect of Crospovidone (%) (X_1) and PVP K30 (%) (X_2) on % CDR at 12 mins. (c) Graph of Actual value vs Predicted value for % CDR at 12 mins.

RESULTS OF STABILITY STUDY

On the basis of all above parameters of Factorial Design batches it was concluded that the batch PSF7 was an optimized batch and stability study was carried out to check the stability of Fast Disintegrating tablets of the Optimized batch at 40°± 2 °C and 75 ± 5% RH for one month. From results of Wetting Time, *In-vitro* Disintegration time, Hardness, Drug Content and Drug Release study as shown in Table 13 and Table 14 shows that there is no significant difference in these parameters. So, it was concluded that selected formulation is stable for longer time period. Comparison study of % Cumulative Drug Release between the result of optimized batch and after time period of stability of optimized batch is graphically illustrated in Figure 16.

Table 13: Result of the Stability study

Evaluation parameter	Results of optimized batch PSF7	Result after 1 month at 40° ± 2 °C and 75 ± 5 % RH
Hardness (kg/cm^3)	2.96 ± 0.055	2.93 ± 0.058
Wetting Time (sec.)	13.54 ± 0.67	13.92 ± 0.14
In-vitro Disintegration Time (sec.)	16.71 ± 0.64	16.84 ± 0.27
% Drug Content	99.16 ± 0.634	99.02 ± 0.77

Table 14: *In-vitro* Drug Release Study for Stability Study of Batch PSF7

Time (Min.)	% CDR of Optimized Batch PSF7 (%)	% CDR of batch PSF7 After Time Period of 1 Month (%)
0	0	0
2	47.58	45.08
4	73.09	70.97
6	90.08	87.56
8	98.21	97.24
10	99.31	98.06
12	99.58	99.12

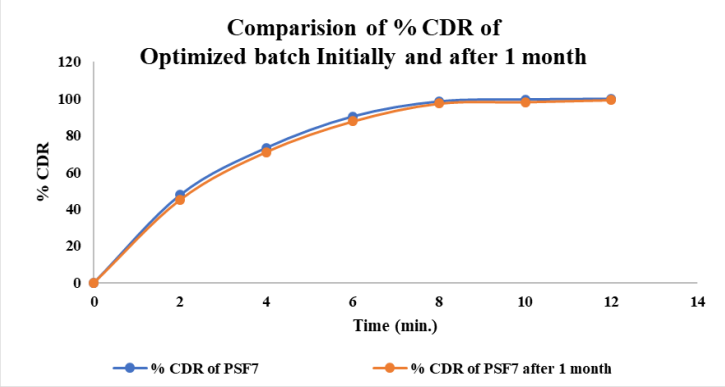

Figure 16: Comparison of *In-vitro* Drug Release study of Optimized batch initially and after 1 month

The stability study of the optimized batch was conducted for one month at accelerated conditions (40 ± 2 °C and 75 ± 5 % RH) to evaluate the effect of storage on critical quality attributes. The results of hardness, Wetting time and *In-vitro* disintegration time exhibited slight reductions after one month, suggesting no adverse impact of storage conditions on rapid tablet performance. Drug content remained within acceptable limits, with values changing minimally confirming chemical stability of the formulation. *In-vitro* drug release profiles before and after one month were found to be comparable across all time points. The % cumulative drug release showed only negligible differences, and more than 99 % drug release was achieved within 12 mins in both cases. The comparative dissolution graph further supports the absence of significant deviation in release behavior after storage. Overall, the stability data confirm that the optimized batch remained physically, chemically, and dissolution-wise stable under accelerated conditions for one month, indicating satisfactory short-term stability of the formulation.

CONCLUSION:

The present study successfully developed and characterized a Pitavastatin–ion exchange resin complex for effective taste masking and desired drug release. Preformulation studies confirmed drug identity and excipient compatibility. Acid-activated Indion 204 at a 1:3 drug-to-resin ratio, pH 5.5, 30°C, with 90 min swelling and 120 min stirring, achieved maximum drug loading of 88.1%. The optimized complex was incorporated into fast disintegrating tablets using a 3^2 full factorial design, with Crospovidone and PVP K30 as independent variables. All formulations met pharmacopeial standards for pre- and post-compression parameters. PSF7 was identified as the optimized batch, demonstrating the lowest wetting time (13.54 sec), fastest disintegration (16.71 sec), and near-complete drug release of 99.58% within 12 minutes. Accelerated stability studies confirmed physical, chemical, and dissolution stability of the optimized formulation over one month, establishing its potential as an effective and patient-compliant oral drug delivery system.

ACKNOWLEDGEMENT:

The authors are grateful to Smt. N. M. Padalia Pharmacy College, Ahmedabad, for encouragement and for providing the necessary facilities to carry out this research work.

CONFLICT OF INTEREST:

The authors declare that there is no conflict of interest.

REFERENCES

1. Attar T and Gharge V, "Review Article on Hyperlipidemia" *International Journal of Pharmaceutical Research and Application.* **2021**; *6(6)*: 468-471. doi: 10.35629/7781-0606468471
2. Nabtity SE, Eleiwa NZ, Kamel MA and Fahmy AA, "Hyperlipidemia: Methods of Induction and Possible Treatments" *Zagazig Veterinary Journal.* **2023**; *51(2)*: 169-184. doi: 10.21608/zvjz.2023.189986.1206
3. Sohi H, Sultana Y and Khar R, "Taste masking technologies in oral pharmaceuticals: Recent developments and approaches." *Drug Development and Industrial Pharmacy*. **2004**; *30(5)*: 429-448. DOI: 10.1081/ddc-120037477
4. Guo X, Chang RK and Hussain MA, "Ion exchange resin as drug delivery carriers." *Journal of Pharmaceutical Sciences*. **2009**; *98*: 3886-3902. doi: 10.1002/jps.21706.
5. Dasari N, Ashok CP and Sudhakar M, "Preparation and characterization of Pitavastatin solid dispersions." *Research Journal of Pharmacy and Technology.* **2016**; *9(5)*: 555-558. doi: 10.5958/0974-360X.2016.00105.0
6. Anand V, Kandarapu R, Garg S. Ion-exchange resins: carrying drug delivery forward. *Current Drug Delivery.* **2001**; *1(3)*: 1–10. doi:10.1016/S1359-6446(01)01922-5
7. Srikanth MV, Sunil SA, Rao NS, Uhumwangho MU, Murthy KVR. Ion-exchange resins as controlled drug delivery carriers. *Journal of Scientific Research.* **2010**; *2(3)*:597–611. doi:10.3329/jsr.v2i3.4991
8. Junlin Y, Conghui Li, Shanshan W, Hui Z, Zengming W, Aiping Z and Xiuli G, Methods and characteristics of drug extraction from ion-exchange resin formulations. *Polymers.* **2023**; *15(5)*:1191. doi:10.3390/polym15051191
9. Conghui L, Xiaolu H, Xiaoxuan H, Xianfu L, Hui Z, Zengming W and Aiping Z, Study on the complexation and release mechanism of drug–resin complexes. *Polymers*. **2021**; *13(24)*:4394. doi:10.3390/polym13244394
10. Dasari N, Maruvajala V. "Preparation and evaluation of fast dissolving tablets of Pitavastatin by 3^2 full factorial design*." International Journal of Applied Pharmaceutics.* **2020**; *12(1)*:108–114. doi: 10.22159/ijap.2020v12i1.35678
11. Kim JI, Cho SM, Cui JH, Cao QR, Oh E, Lee BJ, "In vitro and in vivo correlation of disintegration and bitter taste masking using orally disintegrating tablet containing ion exchange resin–drug complex." *International journal of pharmaceutics.* **2013**; *457(2)*: 342–350. doi: 10.1016/j.ijpharm.2013.07.072
12. Patil SP, Pati AV, Bari MM, Barhate SD, Nasir M. Formulation optimization and evaluation of taste masked oro-dispersible tablet of levocetirizine dihydrochloride by ion exchange resin. *Research Journal of Pharmaceutical Dosage Forms and Technology.* **2022**; *14(4)*:276–282. doi:10.52711/0975-4377.2022.00045
13. Shirsand SB, Suresh S, Swamy PV, Para MS, Nagendra Kumar D. Formulation design of fast disintegrating tablets using disintegrant blends. *Indian Journal of Pharmaceutical Sciences.* **2010**; *72(1)*:130-3. doi: 10.4103/0250-474X.62244.
14. Pharmaceutical composition comprising edoxaban. *WO2012025939A1*. 2012. Google Patents.
15. Mohammad Yunoos, M. Sowjanya, B. Sushma, K. Pavan Kumar. "A Validated Simple UV Spectrophotometric Method for the Estimation of Pitavastatin in bulk and Pharmaceutical Dosage Form." *Asian Journal of Research in Chemistry.* **2014;** *7(4)*:393-396. doi: 10.5958/0974-4150.
16. Aglawe KV, Kharat UP, Dongaonkar CC, Chavan VA. "Development and validation of stability indicating UV spectrophotometric method for the determination of pitavastatin calcium." *World Journal of Pharmacy and Pharmaceutical Sciences.* **2016**; *5(7)*:1773–1787. doi: 10.20959/wjpps20167-7248.
17. Anusha V. & Umashankar MS. & Kumar YG. "Preformulation Studies of Pitavastatin Calcium– A Primary Step in Further Design of Chronotherapeutic Formulation Synchronized with Circadian Rhythm." *International Journal of Drug Delivery Technology*. **2024**; *14(3)*:1578-1585. doi: 10.25258/ijddt.14.3.46.
18. AlKadi H, Alzier A, Mando H, Mando Z, Darwicha JAN, Allaf AW. "Quantitative Determination of Pitavastatin in Tablets Using FTIR and RP-HPLC Analysis: A Comparative Study." *Infect Disord Drug Targets.* **2022**; *22(7)*:49-55. doi: 10.2174/1871526522666220509055847.
19. Jeong SH. and Park K. "Drug loading and release properties of ion-exchange resin complexes as a drug delivery matrix." *International*

Journal of Pharmaceutics. **2008**; *361*: 26–32. doi: 10.1016/j.ijpharm.2008.05.006.
20. **Aglawe KV, Kharat UP, Dongaonkar CC, and Chavan VA.** "Development and validation of stability indicating UV spectrophotometric method for the determination of pitavastatin calcium." WORLD JOURNAL OF PHARMACY AND PHARMACEUTICAL SCIENCES. **2016**; *5(7)*:1773–1787. doi: 10.20959/wjpps20167-7248.
21. Gajji N, Chaitanya MVNL and Satyavathi B. "Design and evaluation of solubility enhancement of poorly soluble drugs using liquid solid compacts." *International Journal of Pharmaceutical Research and Review.* **2015**; *4(10)*: 24–34.
22. Nagotha AV, Ghanchi AH, Chauhan SR, Ansari GY, Raval BA, Bhangale JO, and Patel AD. "Formulation and evaluation of mouth dissolving tablets of Imipramine HCl." *European Journal of Clinical Pharmacology.* **2026**; *8(1)*: 2940–294.
23. Jain P, Gupta RN, and Shrivastava S. "Formulation and evaluation of mouth dissolving tablets of Omeprazole." *International Journal of Current Pharmaceutical Research.* **2016**; *8(2)*: 48–51.
24. Singh S, Shinde R, Rangari N, Gahukar K, and Ingawale S. "Formulation and evaluation of mouth dissolving tablets of Sitagliptin Phosphate with enhanced permeability." *Neuro Quantology*. **2022**; *20(9)*: 5091–5098. doi: 10.14704/nq.2022.20.9.NQ44589.
25. Chatterjee A, Vaghela BJ, Gupta RK, and Ombir. "Formulation and evaluation of mouth dissolving tablets of Montelukast Sodium." *Journal of Biomedical and Pharmaceutical Research.* **2022**; *11(2)*: 31–43. doi: 10.32553/jbpr.v11i2.908.